

Giant nonlinear conduction and thyristor-like negative differential resistance in BaIrO₃ single crystals

Tomohito Nakano* and Ichiro Terasaki†

Department of Applied Physics, Waseda University, 3-4-1 Okubo Shinjuku-ku Tokyo 169-8555, Japan
and CREST, Japan Science and Technology Agency, Kawaguchi, Saitama 332-0012, Japan

(Received 5 September 2005; revised manuscript received 22 February 2006; published 4 May 2006)

We synthesized single-crystalline samples of monoclinic BaIrO₃ using a molten flux method, and measured their magnetization, resistivity, Seebeck coefficient, and nonlinear voltage-current characteristics. The magnetization rapidly increases below the ferromagnetic transition temperature T_C of 180 K, where the resistivity concomitantly shows a hump-type anomaly, followed by a sharp increase below 30 K. The Seebeck coefficient suddenly increases below T_C , and shows linear temperature dependence below 50 K. A most striking feature of this compound is that the anomalously giant nonlinear conduction is observed below 30 K, where a small current density of 20 A/cm² dramatically suppresses the sharp increase in resistivity to induce a metallic conduction down to 4 K.

DOI: 10.1103/PhysRevB.73.195106

PACS number(s): 71.30.+h, 71.45.Lr, 72.15.Jf

An important purpose of condensed matter physics is to understand emergence arising from numerous degrees of freedom. Prime examples are phase transitions and collective excitations: A ferromagnetic transition induces a collective mode of spins known as a magnon, whereas superconductivity lets an electric current flow persistently by spatially changing the phase of the superconducting order parameter. Recent studies of emergence have revealed the importance of competing and/or cooperating orders, in which novel phenomena such as intrinsic inhomogeneity,¹⁻³ quantum criticality,²⁻⁶ and multiferroics⁷⁻⁹ were proposed theoretically, and discovered in real materials.

In the context of competing or cooperating orders, barium iridate BaIrO₃ is of extreme interest. It was synthesized first in the 1960s by Donohue *et al.*¹⁰ It exhibits a charge density wave (CDW) transition accompanying a ferromagnetic transition at the same temperature of $T_C=180$ K.¹¹⁻¹³ The CDW transition was characterized by a hump-type resistivity anomaly and a gaplike optical spectrum.¹¹ The Seebeck coefficient,¹⁴ photoemission,¹⁵ band calculation,¹⁶ and magnetoresistance¹⁷ suggest that a gap is opened in the density of states below T_C . However, a satellite scattering in the x-ray diffraction (XRD) pattern has not yet been reported at present, and thus it needs more discussion whether the gap below T_C can be associated with a conventional CDW or not.

The crystal structure of BaIrO₃ is monoclinic (space group $C2/m$),^{18,19} and contains zigzag chains of the Ir₃O₁₂ trimer with face-shared IrO₆ octahedra along the c axis as shown in Fig. 1. Each trimer is linked to form a corner-shared network along the c axis, and a two-dimensional network perpendicular to the c axis as well. The band calculation revealed a fairly dispersive band along the ab plane as well as along the c axis.¹⁶

We have studied competing or coexisting orders in strongly correlated systems. We found a transition from localized to itinerant antiferromagnetism in the heavy-fermion compound Ce(Ru_{0.85}Rh_{0.15})₂Si₂,²⁰⁻²² and found giant nonlinear conduction in the organic conductor θ -(BEDT-TTF)₂CsM(SCN)₄ [BEDT-TTF

=bis(ethylenedithiolo) tetrathiafulvalene, $M=[\text{Co}, \text{Zn}]$],^{23,24} where two different charge-ordered domains coexist.²⁵ In this paper, we report that BaIrO₃ single crystals exhibit giant nonlinear conduction as a function of pulsed external current, and shows a negative derivative resistance from 2 to 6 A/cm² at 4.2 K. This indicates a collective excitation in solids to be associated with the giant nonlinear conduction in an organic conductor.

Single-crystalline samples of BaIrO₃ with a typical dimension of $1 \times 0.5 \times 0.2$ mm³ were synthesized by the molten flux method using BaCl₂ as solvent. Figure 2(a) shows a typical XRD pattern of a single crystal, where only the sharp peaks for the ($\bar{n}nn$) reflection are observed. The peak width is comparable to the resolution, which indicates the high quality of the single crystals. A typical x-ray diffraction image of a single-crystalline sample is shown in Fig. 2(b), where clear spots also warrant the crystal quality. We further note that all of our samples showed $T_C=180$ K, which is higher than T_C (175 K) of the single crystals prepared

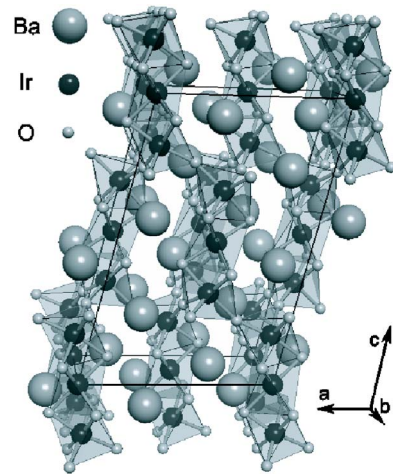


FIG. 1. (Color online) Crystal structure of monoclinic BaIrO₃, which was drawn with VENUS development by Dilanian and Izumi.

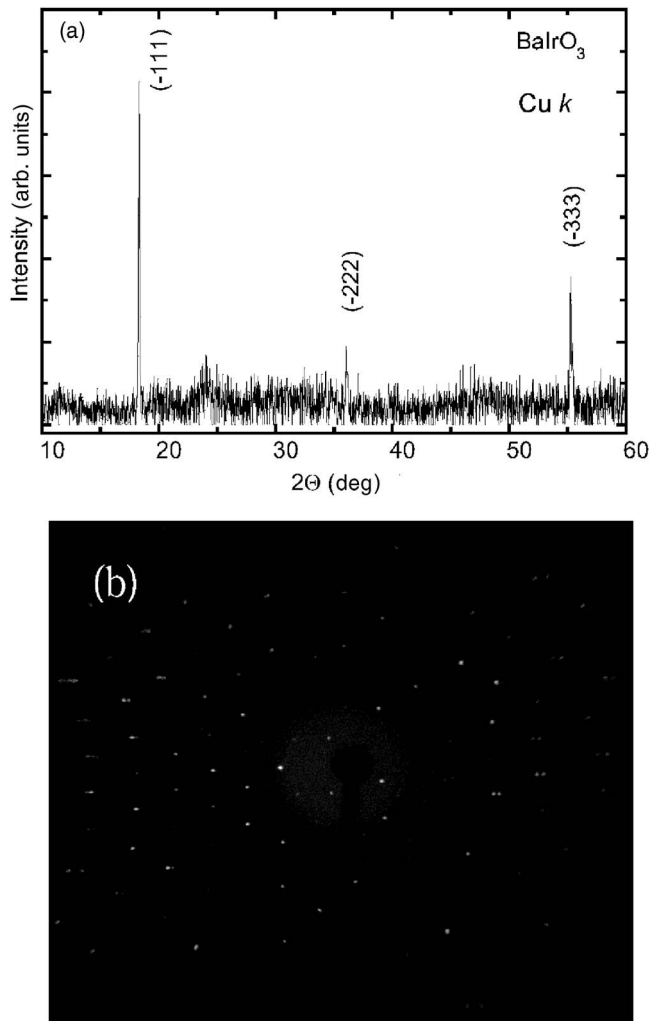


FIG. 2. (a) X-ray diffraction pattern of a BaIrO_3 single crystal for the $(\bar{1}11)$ plane. (b) X-ray diffraction image of a BaIrO_3 single crystal for a certain direction.

previously.¹¹ Since T_C is easily suppressed by impurities,¹⁷ this suggests that our crystals include less disorder.

The magnetization was measured in a magnetic field of 1 kOe with a commercial superconducting quantum interference device magnetometer (Quantum Design). The resistivity was measured by the standard four-probe method in a liquid He cryostat. The voltage-current characteristics were measured on the same sample with a pulsed current of 12 ms using a pulse current source (Keithley 6221) from 4.2 to 120 K. The Seebeck coefficient was measured using a steady-state technique from 4.2 to 300 K in a liquid He cryostat.

The magnetization of a BaIrO_3 single crystal in a magnetic field of 1 kOe parallel and perpendicular to the c axis is shown in Fig. 3(a), exhibiting a rapid increase below $T_C = 180$ K (marked by a vertical arrow in this figure). This is direct evidence for the ferromagnetic transition in this compound. Below about 100 K, the magnetization perpendicular to the c axis is slightly smaller than that parallel to the c axis, indicating that the c axis is the magnetic easy axis.^{11–13} We should note that there is no trace of phase transitions other

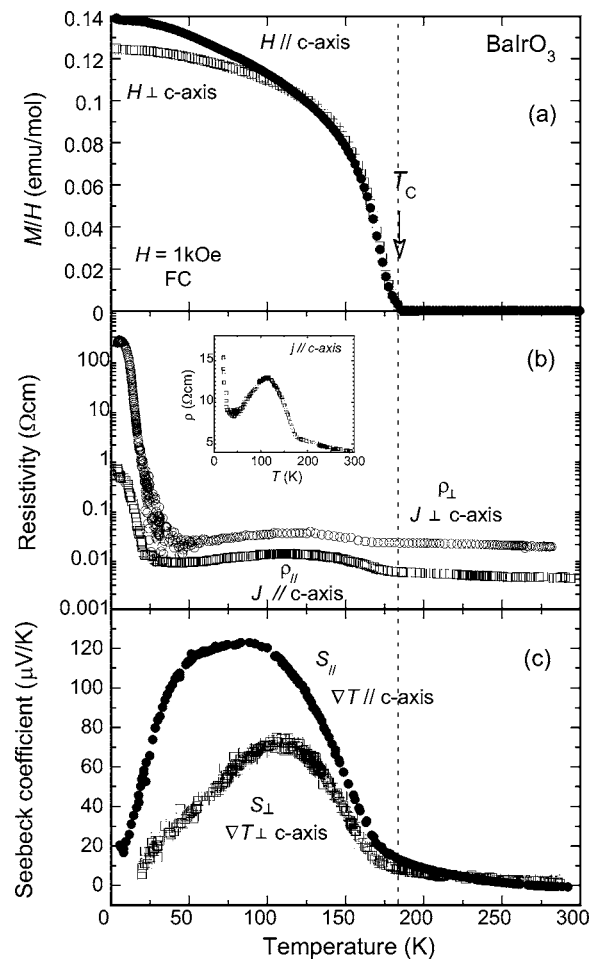


FIG. 3. Temperature dependence of (a) magnetization with magnetic field applied parallel and perpendicular to the c axis, (b) resistivity with external current parallel and perpendicular to the c axis, and (c) Seebeck coefficient with temperature gradient parallel and perpendicular to the c axis. Resistivity with external current parallel to the c axis plotted with a linear scale is shown in the inset of Fig. 3(b).

than at 180 K, which is consistent with the specific heat data.¹⁴

Figure 3(b) shows the resistivity ρ_{\parallel} and ρ_{\perp} for an external current density $J (=0.01 \text{ A/cm}^2)$ parallel and perpendicular to the c axis, respectively. In the inset of Fig. 3(b), we plot the same data for ρ_{\parallel} with a linear scale in order to better show the temperature dependence near T_C , ρ_{\parallel} slightly increases with decreasing temperature from room temperature down to T_C , showing nonmetallic conduction. Then it shows a hump-type anomaly just below T_C , and saturates at around 120 K. The hump implies that a part of the Fermi surface is gapped below T_C . Similar anomalies have been observed in NbSe_3 ,²⁶ Cr ,²⁷ and $\text{Ce}(\text{Ru}_{0.85}\text{Rh}_{0.15})_2\text{Si}_2$.²⁸ Below 120 K, ρ_{\parallel} decreases with decreasing temperature as in a metal. We think that the electric conduction is essentially metallic below T_C , although we cannot see a clear metallic conduction just below T_C where the gap opening dominates ρ_{\parallel} . We may thus say that a “nonmetal-to-metal” transition occurs at the ferromagnetic transition temperature. Below 30 K, ρ_{\parallel} rapidly increases to become 100 times larger from 30 down to 4 K,

which was reported previously.^{11,14} ρ_{\perp} shows similar temperature dependence to ρ_{\parallel} , but the magnitude is about five times larger at room temperature, suggesting that the c -axis zigzag Ir_3O_{12} chain is a predominant conduction path in BaIrO_3 above T_C . On the other hand, $\rho_{\parallel}/\rho_{\perp}$ at 50 K decreases down to 2.5, which indicates that the residual Fermi surface below T_C is more isotropic. Presumably a gap is opened along the chain, and the two-dimensional corner-shared Ir_3O_{12} network becomes effective below T_C .

Figure 3(c) shows the Seebeck coefficient S_{\parallel} and S_{\perp} for the temperature gradient parallel and perpendicular to the c axis, respectively. S_{\parallel} slightly increases with decreasing temperature above T_C , and is suddenly enhanced below T_C to achieve $120 \mu\text{V}/\text{K}$ at 120 K. The sudden increase of S_{\parallel} below T_C is due to a gap opening in the density of states, which is consistent with the hump-type anomaly in ρ_{\parallel} . Below 50 K, S_{\parallel} is roughly linear in temperature T as in a metal, in contrast to the sharp increase of the nonmetallic ρ_{\parallel} . Preliminary data for S_{\perp} (including larger errors than in S_{\parallel} owing to the sample shape) exhibit a similar enhancement due to the gap opening just below T_C and linear temperature dependence below 100 K. A similar temperature dependence of S in a polycrystalline sample was observed by Kini *et al.*¹⁴ Since the Seebeck coefficient is a good probe for entropy per carrier, the T -linear S_{\parallel} and S_{\perp} naturally indicate that the density of states is constant at low temperatures, suggesting no electronic phase transitions below 50 K. Thus the rapid increase in ρ_{\parallel} and ρ_{\perp} below 30 K is unlikely to come from a phase transitions.

A most striking feature of BaIrO_3 is anomalously giant nonlinear conduction at low temperatures, which was first reported by Cao *et al.*¹¹ We measured it more systematically as functions of current and temperature for several samples. We employed pulsed currents, which successfully excluded heating effects, while Cao *et al.* did not state how to avoid heating. They measured the voltage-current characteristics only from 120 to 170 K for $J \perp c$, and only at 9 K for $J \parallel c$. We measured them for both directions at 4.2 K, and further measured the temperature dependence up to 180 K for ρ_{\parallel} .

Figure 4(a) shows the voltage-current characteristics as a function of pulsed current at several temperatures. The electric field E at 4.2 K increases rapidly with increasing current density up to $2 \text{ A}/\text{cm}^2$, above which it decreases abruptly and shows a negative derivative resistance ($dE/dJ < 0$) up to $6 \text{ A}/\text{cm}^2$. Eventually, it becomes Ohmic above $6 \text{ A}/\text{cm}^2$. A similar current dependence at 4.2 K was observed for $J \perp c$ [the inset of Fig. 4(a)]. This giant nonlinear conduction with a “mountain-type” anomaly is suppressed with increasing temperature, and almost disappears above 20 K. The sharp increase in resistivity for $0.01 \text{ A}/\text{cm}^2$ is suppressed by a current density of $20 \text{ A}/\text{cm}^2$, and the resistivity looks metallic down to 4 K for $20 \text{ A}/\text{cm}^2$ as shown in Fig. 4(b).

Now let us compare our data with the data of Cao *et al.*¹¹ First, we did not observe transitions at $T_{C1} = 26 \text{ K}$ and $T_{C2} = 80 \text{ K}$ in ρ_{\parallel} , after having measured ρ_{\parallel} for three different single crystals. The resistivity peak at T_{C2} of their sample might correspond to the resistivity maximum near 120 K seen in Fig. 3(b), at which the metallic conduction in the residual Fermi surface competes with the resistivity enhance-

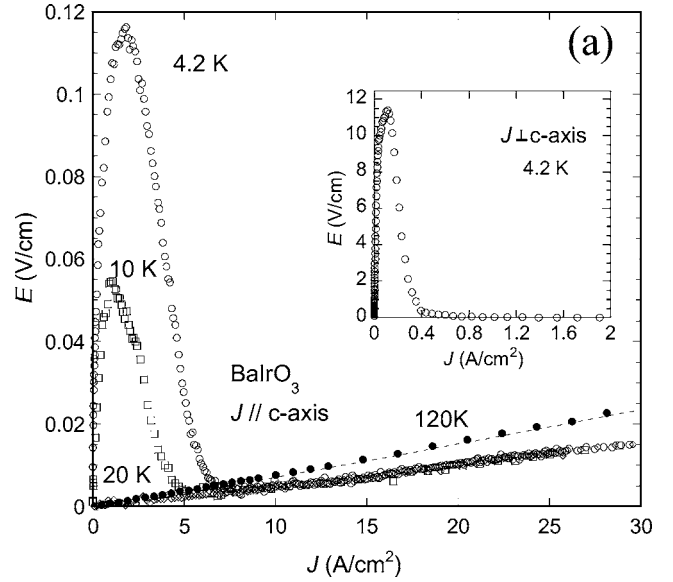


FIG. 4. (a) Nonlinear voltage-current characteristics with pulsed current (pulse width 12 ms) along the c axis at the several temperatures. Dashed line is a guide to eye. In the inset are shown nonlinear voltage-current characteristics perpendicular to the c axis at 4.2 K. (b) The temperature dependence of resistivity for $J = 0.02$ [the same J for the data in Fig. 3(b)] and $20 \text{ A}/\text{cm}^2$ along the c axis.

ment due to the gap opening. The sudden drop at $T_{C1} = 26 \text{ K}$ should be associated with giant nonlinear conduction. We should emphasize that we simultaneously measured S_{\perp} and S_{\parallel} , which is a good probe for entropy per carrier. No anomalies in S_{\perp} and S_{\parallel} below T_C strongly suggest no transitions at T_{C1} and T_{C2} . Second, Cao *et al.* observed nonlinear conduction for $J \perp c$ from 120 to 170 K, whereas we observed no appreciable nonlinear conduction above 30 K. Self-heating could give a similar nonlinear conduction. Third, our E - J characteristics for $J \parallel c$ are much more drastic than theirs: Through the negative resistance region, E/J of our sample decreases by a factor of 100, while E/J of their sample decreases by a factor of 2.

The E - J characteristics are qualitatively similar to those of a thyristor.²⁴ As is well known, the thyristor is an electronic component consisting of two pairs of p - n diodes, and the nonlinear conduction is based on the interface effects at the p - n junctions. In contrast, the nonlinear conduction of BaIrO_3 is a *bulk* effect: This is observed in the four-probe configuration where the voltage drop is far from the interface at the current contact. We further note that the characteristic field ($0.12 \text{ V}/\text{cm}$ at 4.2 K) is extremely low, which clearly excludes the possibility for hot electron and/or impact ionization. In such systems, a nonlinear response may occur, when the electric energy gained by the applied electric field E exceeds the thermal energy $k_B T$. Then a characteristic length scale L can be defined by $eEL = k_B T$. L is estimated to be $30 \mu\text{m}$ at 4.2 K for $0.12 \text{ V}/\text{cm}$, which is much longer than the electron mean free path. Thus some other physics is required to explain the observed nonlinear conduction.

We do not think that the sliding motion of the CDW is the origin for the nonlinear conduction in BaIrO_3 for the following reasons. (i) The giant nonlinear conduction occurs only

below 20 K, well below $T_C=180$ K. As already mentioned, no trace of phase transitions is detected in the susceptibility and the specific heat below 180 K. Nonlinear conduction would be seen for a CDW conductor at any temperature below T_C , which implies that it is not related to the CDW transition. (ii) The nonlinear conduction was observed along both the directions parallel and perpendicular to the c axis. A CDW conductor would show nonlinear conduction only along the nesting vector, and would retain ohmic conduction in the other two directions. (iii) The E - J characteristics are different from those of a CDW conductor. The latter shows an abrupt jump in resistivity at a certain threshold electric field, and rarely shows such a clear negative derivative resistance.²⁹

Instead of a CDW, we propose three possible scenarios for the giant nonlinear conduction. The first one is due to competition between the ferromagnetic and charge-gapped domains. Suppose that ferromagnetic domains are separated from the charge-gapped domains in space. Then the former domains grow and squeeze the latter domains at low temperatures, and eventually break them into fragments. In such a situation, the electric conduction is dominated by a percolation network of fragmented domains, where the nonlinear conduction is realized by rearrangement of the percolative conduction path with external currents. The second one is an "electron liquid crystal,"³⁰ where charge stripes are formed below T_C , and an isotropic-nematic crossover occurs below 30 K. An external current would wash away the nematic order to cause nonlinear conduction. The third one is based on interplay between two different bands. According to the band calculation,¹⁶ one- and two-dimensional bands characterized by different nesting vectors cross the Fermi energy. As already mentioned, the resistivity ratio $\rho_{\perp}/\rho_{\parallel}$ changes from 5 to 2.5 at T_C . This suggests that a gap opens in the one-dimensional band at T_C , and the two-dimensional band remains ungapped. The Fermi-surface nesting in the two-dimensional band then increases at low temperatures, but cannot attain long-range order because of the incompatible nesting vectors. This resembles the competing charge orders in the organic thyristor θ -(BEDT-TTF)₂CsM(SCN)₄,^{23,24} where two kinds of charge-ordered nanodomains coexist at low temperatures.²⁵

Although further study is necessary, we prefer the third scenario. In the first scenario it is difficult to explain the fact that the nonlinear conduction and T_C are independent of external magnetic field up to 10 T (not shown). The second scenario should indicate that the transport properties of BaIrO₃ are qualitatively different from those of the stripe phase in the high-temperature superconductor.³¹ As for the third scenario, one can find that the features (i), (ii), and (iii) are commonly seen in BaIrO₃ and θ -(BEDT-TTF)₂CsM(SCN)₄. A recent muon-spin resonance measurement reveals a local rearrangement of the magnetic moments below 26 K,³² which could be associated with competing gapped phases. A careful diffraction study with external currents is of course indispensable and is now in progress.

In summary, single-crystalline samples of monoclinic BaIrO₃ were synthesized using the flux method, and their magnetization, resistivity, Seebeck coefficient, and nonlinear voltage-current characteristics were measured. The magnetizations with a field parallel and perpendicular to the c axis show a rapid increase due to ferromagnetic ordering below T_C of 180 K. The resistivity along the c axis shows a non-metallic conduction above T_C and a metallic behavior from 120 down to 30 K, through a hump-type anomaly corresponding to a gap opening in the density of states just below T_C . Finally it exhibits a sharp increase below 30 K, which is highly nonlinear for external currents. The Seebeck coefficient suddenly increases below T_C , and is in proportion to temperature like a metal below 50 K. Anomalous giant nonlinear conduction is observed below 20 K, and metallic conduction is induced with disappearance of the sharp increase below 30 K by a current density of 20 A/cm². A quantitative comparison with the nonlinear conduction of a charge density wave has revealed that the giant nonlinear conduction in BaIrO₃ belongs to a different class of collective excitations in solids.

The authors would like to thank A. J. Schofield for valuable discussion on electron liquid crystals. They appreciate Y. Nogami, N. Ikeda, and K. Yubuta for collaboration on diffraction measurements.

*FAX: +81-3-5286-3854. Email address: nakano@htsc.sci.waseda.ac.jp.

†FAX: +81-3-5286-3854. Email address: terra@waseda.jp.

¹J. Burgy, M. Mayr, V. Martin-Mayor, A. Moreo, and E. Dagotto, Phys. Rev. Lett. **87**, 277202 (2001).

²K. M. Lang, V. Madhavan, J. E. Hoffman, E. W. Hudson, H. Eisaki, S. Uchida, and J. C. Davis, Nature (London) **415**, 412 (2002).

³M. Uehara, S. Mori, C. H. Chen, and S.-W. Cheong, Nature (London) **399**, 560 (1999).

⁴I. Paul and G. Kotliar, Phys. Rev. B **64**, 184414 (2001).

⁵P. van Dongen, K. Majumdar, C. Huscroft, and F. C. Zhang, Phys. Rev. B **64**, 195123 (2001).

⁶P. Coleman and A. J. Schofield, Nature (London) **433**, 226

(2005).

⁷J. Wang *et al.*, Science **299**, 1719 (2003).

⁸T. Kimura, T. Goto, H. Shintani, K. Ishizaka, T. Arima, and Y. Tokura, Nature (London) **426**, 55 (2003).

⁹N. Hur, S. Park, P. A. Sharma, J. S. Ahn, S. Guha, and S.-W. Cheong, Nature (London) **429**, 392 (2004).

¹⁰P. C. Donohue, L. Katz, and R. Ward, Inorg. Chem. **4**, 306 (1965).

¹¹G. Cao, J. E. Crow, R. P. Guertin, P. F. Henning, C. C. Homes, M. Strongin, D. N. Basov, and E. Lochner, Solid State Commun. **113**, 657 (2000).

¹²B. L. Chamberland, J. Less-Common Met. **171**, 377 (1991).

¹³R. Lindsay, W. Strange, B. L. Chamberland, and R. O. Moyer Jr., Solid State Commun. **86**, 759 (1993).

- ¹⁴N. S. Kini, A. Bientien, S. Ramakrishnan, and C. Geibel, *Physica B* **359-369**, 1264 (2005).
- ¹⁵K. Maiti, R. S. Singh, V. R. R. Medicherla, S. Rayaprol, and E. V. Sampathkumaran, *Phys. Rev. Lett.* **95**, 016404 (2005).
- ¹⁶M.-H. Whangbo and H.-J. Koo, *Solid State Commun.* **118**, 491 (2001).
- ¹⁷G. Cao, X. N. Lin, S. Chikara, V. Durairaj, and E. Elhami, *Phys. Rev. B* **69**, 174418 (2004).
- ¹⁸P. L. Gai, A. J. Jacobson, and C. N. R. Rao, *Inorg. Chem.* **15**, 480 (1976).
- ¹⁹T. Siegrist and B. L. Chamberland, *J. Less-Common Met.* **170**, 93 (1991).
- ²⁰T. Nakano, H. Yamashiro, K. Fujita, and S. Murayama, *J. Phys. Soc. Jpn.* **74**, 1602 (2005).
- ²¹T. Nakano, K. Fujita, Y. Ohmori, S. Murayama, K. Hoshi, H. Amitsuka, Y. Onuki, M. Ocio, and J. Hammann, *Physica B* **312-313**, 440 (2002).
- ²²A. Isoda, S. Shimada, Y. Kanda, S. Murayama, H. Takano, T. Nakano, M. Hedo, and Y. Uwatoko, *Physica B* **359-361**, 169 (2005).
- ²³K. Inagaki, I. Terasaki, H. Mori, and T. Mori, *J. Phys. Soc. Jpn.* **73**, 3364 (2004).
- ²⁴F. Sawano, I. Terasaki, H. Mori, T. Mori, M. Watanabe, N. Ikeda, Y. Nogami, and Y. Noda, *Nature (London)* **437**, 522 (2005).
- ²⁵M. Watanabe, Y. Nogami, K. Oshima, H. Mori, and S. Tanaka, *J. Phys. Soc. Jpn.* **68**, 2654 (1999).
- ²⁶P. Monceau, N. P. Ong, A. M. Portis, A. Meerschaut, and J. Rouxel, *Phys. Rev. Lett.* **37**, 602 (1976).
- ²⁷E. Fawcett, *Rev. Mod. Phys.* **60**, 209 (1988).
- ²⁸S. Murayama, C. Sekine, A. Yokoyanagi, K. Hoshi, and Y. Onuki, *Phys. Rev. B* **56**, 11092 (1997).
- ²⁹G. Gruner, *Density Waves in Solids* (Addison-Wesley Longmans, Reading, 1994).
- ³⁰S. A. Kivelson, E. Fradkin, and V. J. Emery, *Nature (London)* **393**, 550 (1998).
- ³¹Y. Ando, K. Segawa, S. Komiya, and A. N. Lavrov, *Phys. Rev. Lett.* **88**, 137005 (2002).
- ³²M. L. Brooks, S. J. Blundell, T. Lancaster, W. Hayes, F. L. Pratt, P. P. C. Frampton, and P. D. Battle, *Phys. Rev. B* **71**, 220411(R) (2005).